

Contract No:

This document was prepared in conjunction with work accomplished under Contract No. DE-AC09-08SR22470 with the U.S. Department of Energy.

Disclaimer:

This work was prepared under an agreement with and funded by the U.S. Government. Neither the U. S. Government or its employees, nor any of its contractors, subcontractors or their employees, makes any express or implied: 1. warranty or assumes any legal liability for the accuracy, completeness, or for the use or results of such use of any information, product, or process disclosed; or 2. representation that such use or results of such use would not infringe privately owned rights; or 3. endorsement or recommendation of any specifically identified commercial product, process, or service. Any views and opinions of authors expressed in this work do not necessarily state or reflect those of the United States Government, or its contractors, or subcontractors.

Thermodynamics of Partially Frozen Cooling Lakes

Alfred J. Garrett^{*a}, May Casterline^b, Carl Salvaggio^b
^aSavannah River National Laboratory, Highway 1, Aiken SC
^bRochester Institute of Technology, Rochester, NY USA

ABSTRACT

The Rochester Institute of Technology (RIT) collected visible, SWIR, MWIR and LWIR imagery of the Midland (Michigan) Cogeneration Ventures Plant from aircraft during the winter of 2008 – 2009. RIT also made ground-based measurements of lake water and ice temperatures, ice thickness and atmospheric variables. The Savannah River National Laboratory (SRNL) used the data collected by RIT and a 3-D hydrodynamic code to simulate the Midland cooling lake. The hydrodynamic code was able to reproduce the time distribution of ice coverage on the lake during the entire winter. The simulations and data show that the amount of ice coverage is almost linearly proportional to the rate at which heat is injected into the lake (Q). Very rapid melting of ice occurs when strong winds accelerate the movement of warm water underneath the ice. A snow layer on top of the ice acts as an insulator and decreases the rate of heat loss from the water below the ice to the atmosphere above. The simulated ice cover on the lake was not highly sensitive to the thickness of the snow layer. The simplicity of the relationship between ice cover and Q and the weak responses of ice cover to snow depth over the ice are probably attributable to the negative feedback loop that exists between ice cover and heat loss to the atmosphere.

Keywords: power plant, cooling lake, thermal imagery, ice formation, heat transfer, snow insulation

1. INTRODUCTION

Power plant cooling lakes are normally evaluated under extreme heat conditions, which can force reductions in electricity generation. In extremely cold winter weather, power plant cooling lakes may partially freeze, which provides an opportunity to use remote sensing to learn about cooling lake circulation patterns and heat transfer. A cooling lake that is receiving large amounts of waste heat from a power plant in extremely cold weather provides a rigorous test of hydrodynamic and thermodynamic simulation codes, because there is a sudden transition from strong heat transfer over the unfrozen part of the lake surface to poor heat transfer over the frozen part of the lake surface that is exacerbated by an insulating layer of snow. It can be surmised that the amount of ice cover will be a function of the severity of the cold and the rate at which heat is discharged to the lake. The functional relationship between these two independent variables and the amount of ice cover cannot be predicted in advance because the hydrodynamics and thermodynamics of a cooling lake are so complex in these conditions. Aside from the discontinuity in heat transfer that occurs at the ice – water boundary, thermal stratification in the liquid water will reverse from the typical warmer water over colder water near the hot water discharge to a reverse stratification (cold water over warmer water) in the colder parts of the lake. The reverse stratification occurs at the point where water temperatures have dropped below 4°C, which is the temperature at which fresh water is densest.

This paper presents the current results of an investigation by SRNL and RIT of the hydrodynamics and thermodynamics of the Midland (Michigan) Cogeneration Ventures (MCV) Plant. Figure 1 is an aerial photo of the MCV Plant and its cooling lake taken when no ice was present. MCV discharges waste heat into the cooling lake at a rate that typically ranges from 200 to 500 MW. This is a fairly small heat load for a cooling lake with a surface area of 3.7 km² (880 acres). For this reason, the MCV cooling lake is more prone to partial freezing in the winter relative to cooling lakes receiving higher heat loads per unit area.

The objective of the research is to derive quantitative relationships between variables that characterize the ice cover such as total area covered and ice thickness and the variables that control the amount of ice present on the lake, including severity of weather, rate of waste heat discharge into the lake and thickness of snow cover on the ice.

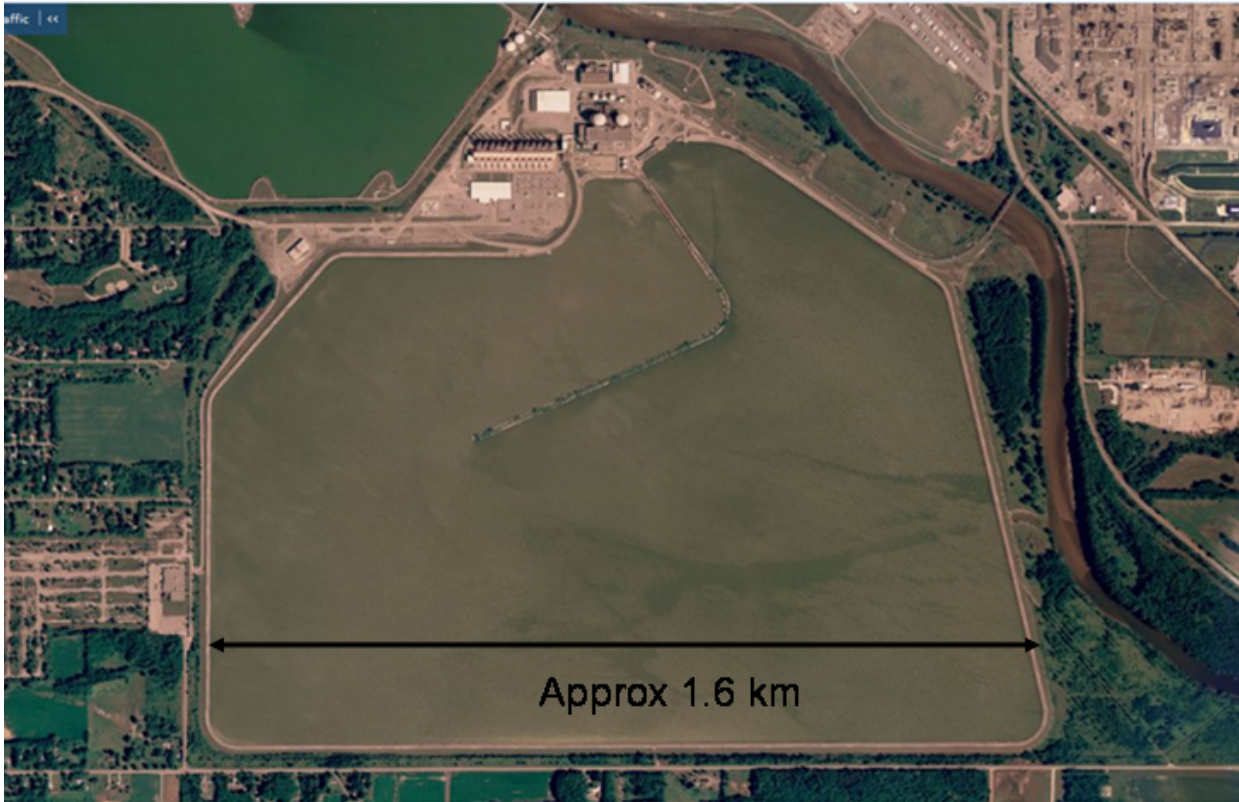


Fig. 1. This visible image of the Midland Cogeneration Ventures (MCV) Power Plant shows the cooling lake when no ice is present. The berm that extends down from the upper part of the lake forces heated discharge water to spread over the entire lake surface before it is drawn into the cooling water intake.

2. DATA COLLECTIONS

RIT's data campaign for the winter of 2008-2009 was segmented into two major branches: the aerial data collection and the ground truth collection. RIT's Wildfire Airborne Sensor Program (WASP) sensor is a multi-spectral aerial mapping system with broad band coverage in the infrared and visible spectrum. Built by the RIT Laboratory for Imaging Algorithms and Systems (LIAS), WASP utilizes direct georeferencing hardware and processing techniques to create orthorectified imagery on-the-fly as the sensor is flown over the target scene. WASP was built with three 640x512 pixel infrared cameras covering $0.9\mu\text{m} - 1.7\mu\text{m}$, $3\mu\text{m} - 5\mu\text{m}$ and $8\mu\text{m} - 9.2\mu\text{m}$; this spectral coverage allows the use a multi-spectral technique for positively detecting the presence of a wildfire in the imaged scene. Each infrared (IR) camera has a 25 micron pixel pitch and a lens with an approximate focal length of 25mm. The system also carries a 4096x4096 pixel RGB camera with a 9 micron pixel pitch and 50mm lens which provides higher resolution visual coverage of the mission area.

While the aerial data collection has a single node of collection, the ground truth collection was a multi-faceted venture involving both manual and automatic measurements of water surface temperature, ice thickness, and weather conditions. Five buoys were deployed in the cooling lake of the Midland Cogeneration Venture (MCV) located in Midland, Michigan, while a weather station was constructed on the shore. The buoys as well as the weather station took automatic measurements of various parameters of interest and transmitted the data on daily intervals via cellular modems. In

addition to the constant monitoring provided by the buoys, manual, high-density surface temperature measurements and ice thickness measurements were taken immediately following imagery collects. Flights were attempted on a weekly interval, as weather permitted.

The airborne imagery collection was augmented by ground-based imaging in which a camera mounted on top of a building adjacent to the lake was used to photograph the lake. RIT developed an image processing technique to derive lake ice coverage from the photos. The airborne and ground-based data collections are described in detail in Reference 1.

3. HYDRODYNAMIC SIMULATIONS

The ALGE code was developed to be a surface water system simulation code that is applicable to a wide range of surface water flow problems. ALGE has been used to simulate power plant cooling lakes, pollutant discharges to rivers, ocean discharges, radioactivity fate and transport in estuaries and sediment transport in large lakes^{2,3,4,5,6}. In this project, SRNL added a one-dimensional ice simulation model⁷ to the ALGE code and developed the logic required to integrate the ice model into a 3-D hydrodynamic code. Some additional functions relating to ice properties were taken from References 8 and 9. Figure 2 shows a sequence of images from an ALGE simulation of the Midland Power Plant cooling lake that starts in the early fall with ice-free conditions (Figure 2a) and progresses to the mid-winter when most of the lake is covered by ice except for a small region close to the hot water discharge (Figure 2d).

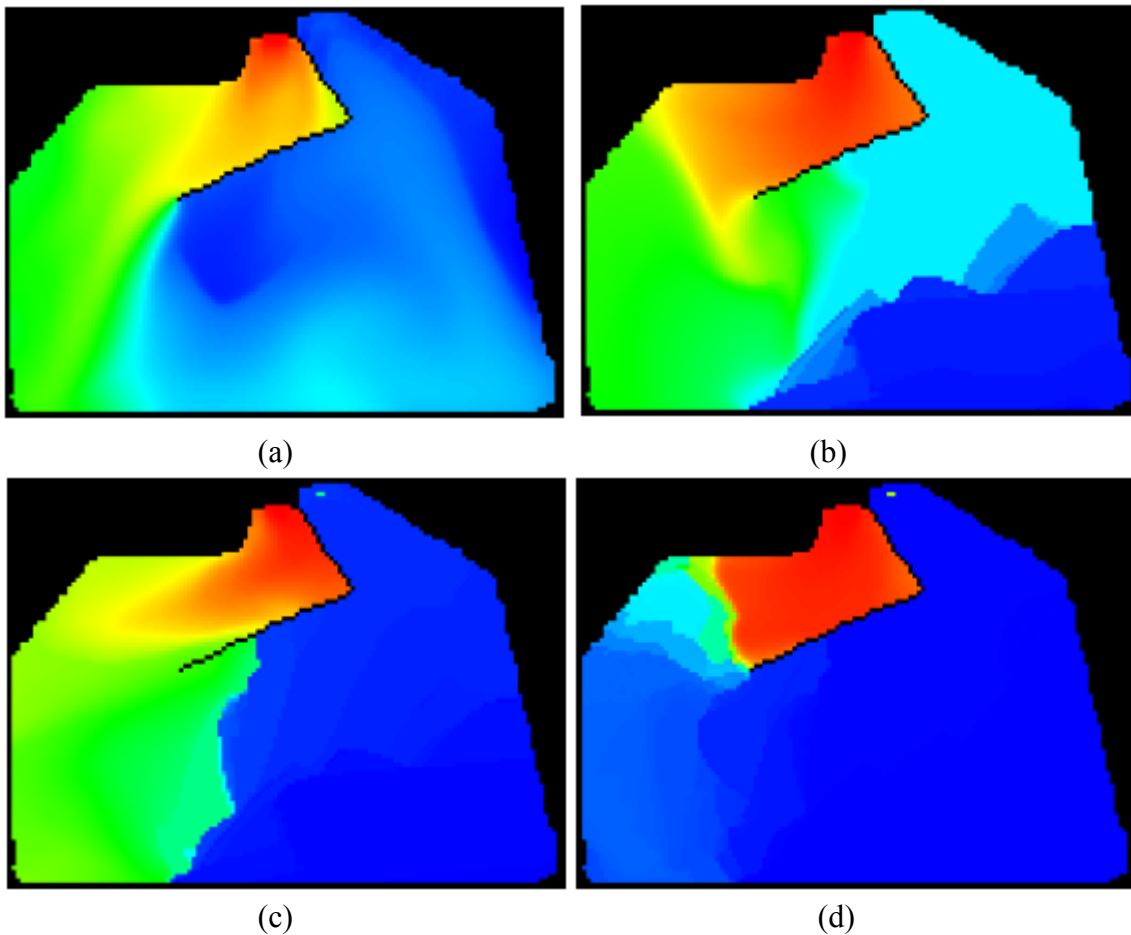


Fig. 2. Sequence of thermal images generated from simulation by ALGE code showing surface temperatures starting in early fall with ice-free lake (a), progressing through steadily increasing ice cover (b, c) to midwinter, when most of the lake is ice-covered except for a small area near the hot water discharge (d). Simulated ice cover in frames (b) – (d) is within jagged dark blue areas.

The primary variable for model assessment is the measured ice-free area of the lake, or equivalently, the ice-covered portion of the lake. During the 2008 – 2009 winter data collections, RIT produced a data base of 16 days on which it estimated ice coverage on the Midland Power Plant cooling lake. The dates and percent of the lake covered by ice are summarized in Table 1 below:

Table 1: 2008 – 2009 Measured Percent Ice Cover on Midland Cooling Lake

date	percent coverage
12/18/08	72
1/14/09	95
1/15/09	90
1/26/09	75
02/02/09	52
2/3/09	69
2/4/09	59
2/5/09	75
2/6/09	67
2/9/09	44
2/10/09	44
2/16/09	5
2/24/09	91
2/25/09	71
3/4/09	56
3/13/2009	0

The sixteenth day in Table 1 (March 13, 2009) was added to show the date on which RIT observed that all ice cover was gone from the lake for the 2008 – 2009 collection period. Table 1 combines ice cover estimates derived from images taken from aircraft and ground-based images. The estimate for February 16, 2009 was based on visual observations by RIT personnel present, who saw only patches of floating ice amounting to a few percent of the total lake surface area. Unfortunately, no observations were available before December 18, 2008, when most of the lake was already covered by ice.

The presence of snow in simulations of partially frozen cooling lakes has a significant impact on the predicted ice thickness, because snow is an effective insulator which reduces heat losses from the water below the ice to the atmosphere above. The thermal conductivity, density and heat capacity are well-known and can be modeled accurately. The same properties for snow are much more uncertain, because the density and physical properties of snow are highly variable. Fresh powder has much lower density, heat capacity and thermal conductivity than old snow that has partially melted and refrozen. It was not possible for RIT to make meaningful measurements of snow thermodynamic or radiation properties partially due to budget constraints and partially because the variety of possible snow conditions is so large. For this reason, SRNL decided to treat snow depth on top of the ice layer as an uncertainty variable, and determine how large the uncertainty is as a function of input snow depth. The ALGE simulations did vary the thermodynamic properties of the input snow layer as a function of temperature, using the functions given in Reference 7.

Figure 3 shows the results of 4 simulations that use two different snow depths (3 cm and 10 cm) and two different models for downwelling thermal radiation. The Kondratyev model¹⁰ is a 1-D lumped waveband model that solves the basic radiative transfer equations for a horizontally homogeneous atmosphere. Garrett (unpublished notes) added the option to include a blackbody cloud layer at a prescribed elevation to the model. The Maykut and Church model⁹ is purely empirical and is a function of only the surface air temperature (about 1.5 m above surface) and the percentage of the sky obscured by clouds (cloud height not considered). The 16 estimates of ice cover by RIT in Table 1 are also shown in Figure 3.

It can be seen that all of the different combinations of downwelling thermal radiation models and snow depths produce ice coverage that tracks the measurements. The simulations that used 10 cm of snow cover produced somewhat better

agreement with the measurements than the simulations that used 3 cm of snow, although the differences are small. For example, the simulation that used the empirical downwelling thermal radiation model (emp LWIR) and 3 cm of snow predicted an average ice cover of 60% versus the measured average of 64%. The simulation that used emp LWIR and 10 cm of snow produced the average measured 64% average ice cover. The simulation that used the 1D downwelling thermal radiation model (1D LWIR) and 10 cm of snow predicted an average ice cover of 70%.

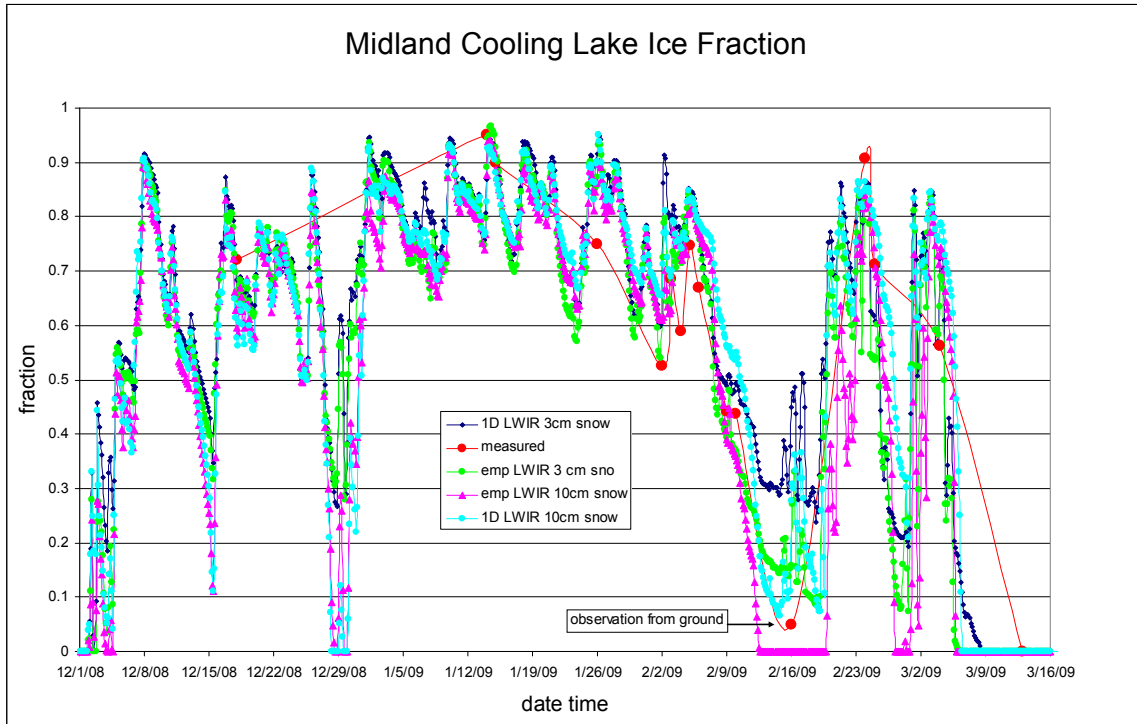


Fig. 3. Comparison of 4 simulations of Midland cooling lake to measured ice coverage during 2008 – 2009 winter data collection period. Results are shown from simulations that used two different downwelling thermal radiation models (emp LWIR and 1D LWIR) and two different input snow depths 3 cm sno and 10 cm sno).

Figure 4 shows the correlation between the measured and simulated ice cover for the two simulations that used 10 cm of snow cover (emp LWIR and 1D LWIR). The overall performance of the simulation that used the emp LWIR model was better, with a higher R^2 value, a slope of 1.0 and an intercept close to zero (Figure 4a). The corresponding statistics for the simulation that used 1D LWIR are not as good (Figure 4b). The slightly better performance of the emp LWIR simulation is unexpected, because the 1D LWIR model uses atmospheric profiles of temperature and humidity and it incorporates the blackbody behavior of clouds at the temperature of the atmosphere where clouds were observed. In other (unpublished) work SRNL found that the 1D LWIR model is more accurate than empirical LWIR models. The emp LWIR model only uses surface temperatures and cloud cover but not cloud height. The emp LWIR model apparently produced better agreement with measured ice cover because it was developed specifically from cold climate data⁹.

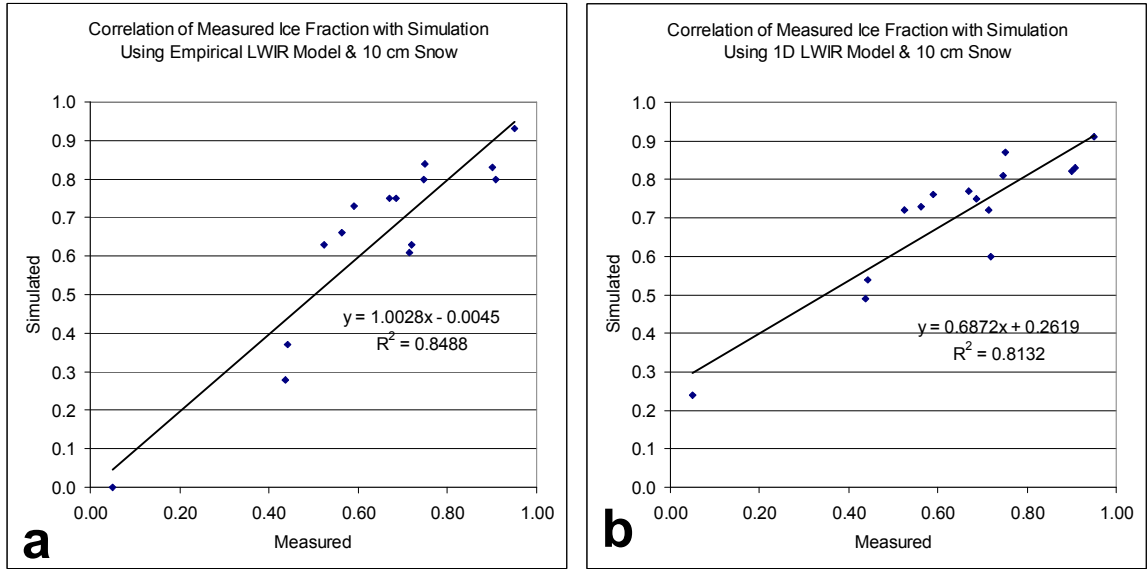


Fig. 4. Correlation between measured and simulated ice cover for simulations using (a) empirical LWIR model and (b) 1D LWIR model.

The differences between the emp LWIR and 1D LWIR are explored in Figure 5, which plots measured downwelling thermal radiation and the computed values from the two models. Although the average difference is small, the average flux computed with the emp LWIR model is closer to the averaged measured value. This difference is not apparent when the time series of measured and computed fluxes are examined. As a practical matter, the emp LWIR model is preferred, because profiles of temperature and humidity are not needed to run the simulations that use it to estimate the downwelling thermal radiation flux.

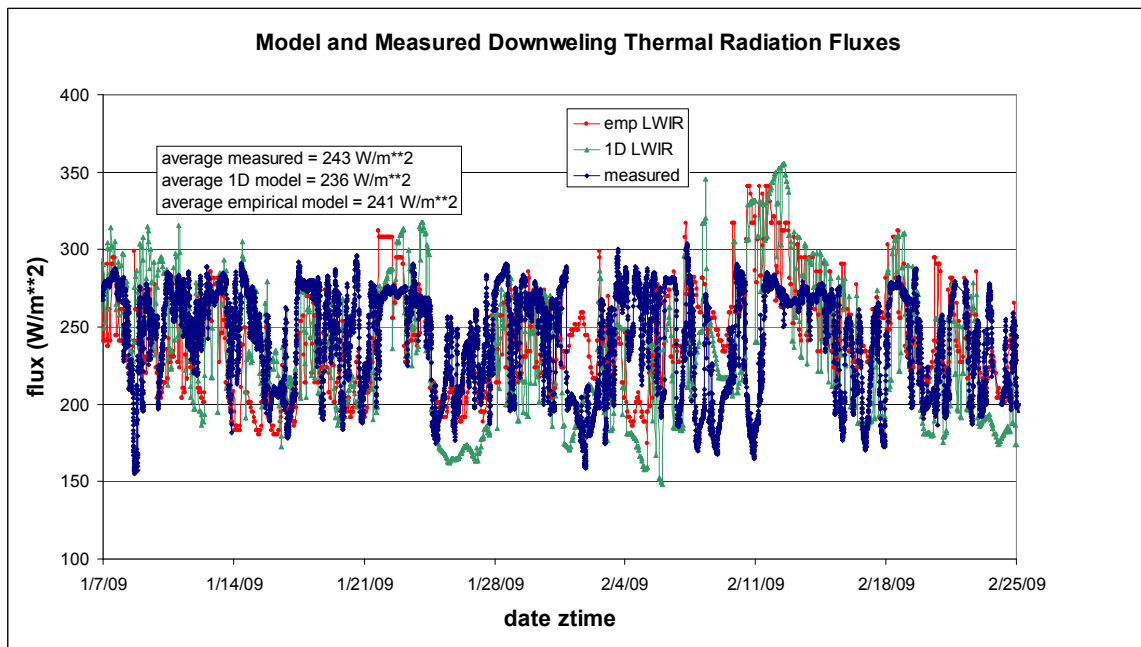


Fig. 5. Measured and computed downwelling thermal radiation for several weeks during January and February 2009. Curve identified as emp LWIR is an empirical model and 1D LWIR is a one-dimensional lumped waveband model. Measurements were made by RIT at station immediately adjacent to lake.

Figure 6 compares measured solar flux to values computed by the ALGE solar radiation module from early January to March 2009. This figure illustrates the difficulties in attempting to calculate instantaneous solar radiation flux using hourly observed cloud cover. There are several days on which the midday measured solar flux is clearly higher than the computed flux, but the average computed flux is higher than the average measured flux (89 Wm^{-2} versus 79 Wm^{-2} computed). The high midday spikes in measured solar radiation are attributed to conditions in which the sun was shining directly on the pyrhelimeter and reflection of solar radiation off nearby clouds was also occurring. It is not clear at this time whether the apparent positive bias in the ALGE solar module had on the ice simulations. The 10 Wm^{-2} positive bias of the ALGE solar module must have more than compensated for the -5 Wm^{-2} bias of the 1D LWIR model.

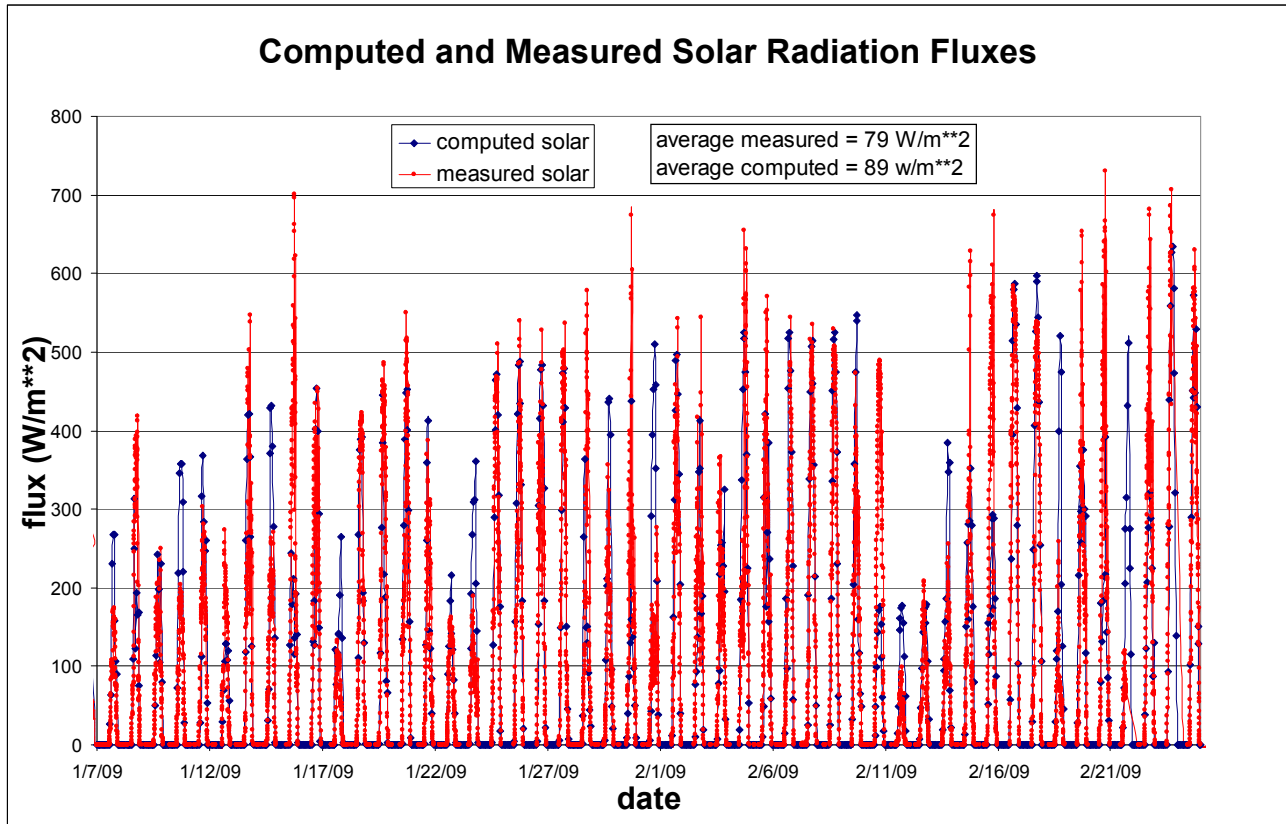


Fig. 6. Measured and calculated solar fluxes from early January to March, 2009 at Midland power plant. Spikes in midday solar fluxes on some days are attributed to direct solar transmission to sensor plus reflected solar radiation off adjacent clouds.

Figure 7 compares measured and computed solar fluxes for several days in late February and early March, 2009. It can be seen that there is excellent agreement between measured and calculated fluxes on clear days. There are no spikes in the measured solar fluxes on the completely clear days. The deficiencies in the hourly cloud cover data (reported from closest National Weather Service station) are apparent on the other days. The NWS cloud cover data does not include cloud type, which precludes use of solar transmission functions based on cloud type. The ALGE solar module assumes stratocumulus when the reported cloud cover is greater than 50% and cumulus when it is less than 50%.

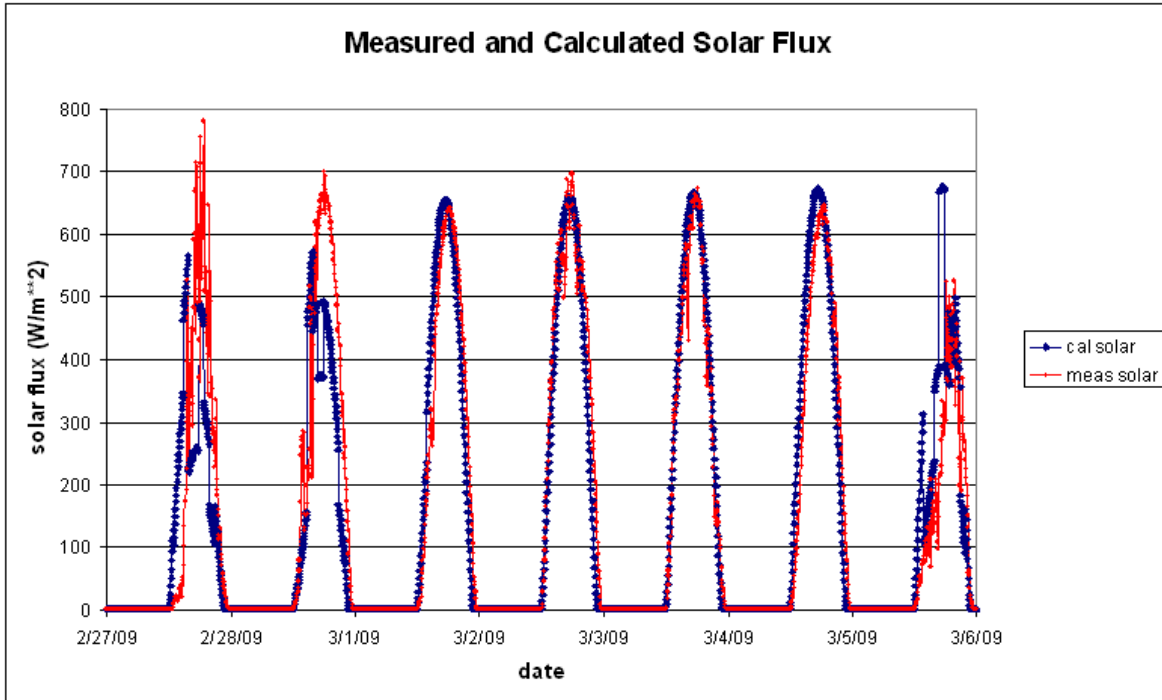


Fig. 7. Measured and calculated solar fluxes during several days in late February and early March, 2009. Agreement is excellent on clear days.

Figure 8 compares measured and computed solar fluxes for several days in January 2009. The maximum measured and computed fluxes are much lower than in Figure 21, illustrating one of the reasons for the rapid and permanent decline in ice cover apparent in Figure 3 in early March. There were a few scattered clouds during the second, third and fourth days shown in Figure 8. Those scattered clouds produced spiking in the measured solar fluxes on those days (higher than the maximum computed fluxes), which did not occur on the completely clear days in Figure 7.

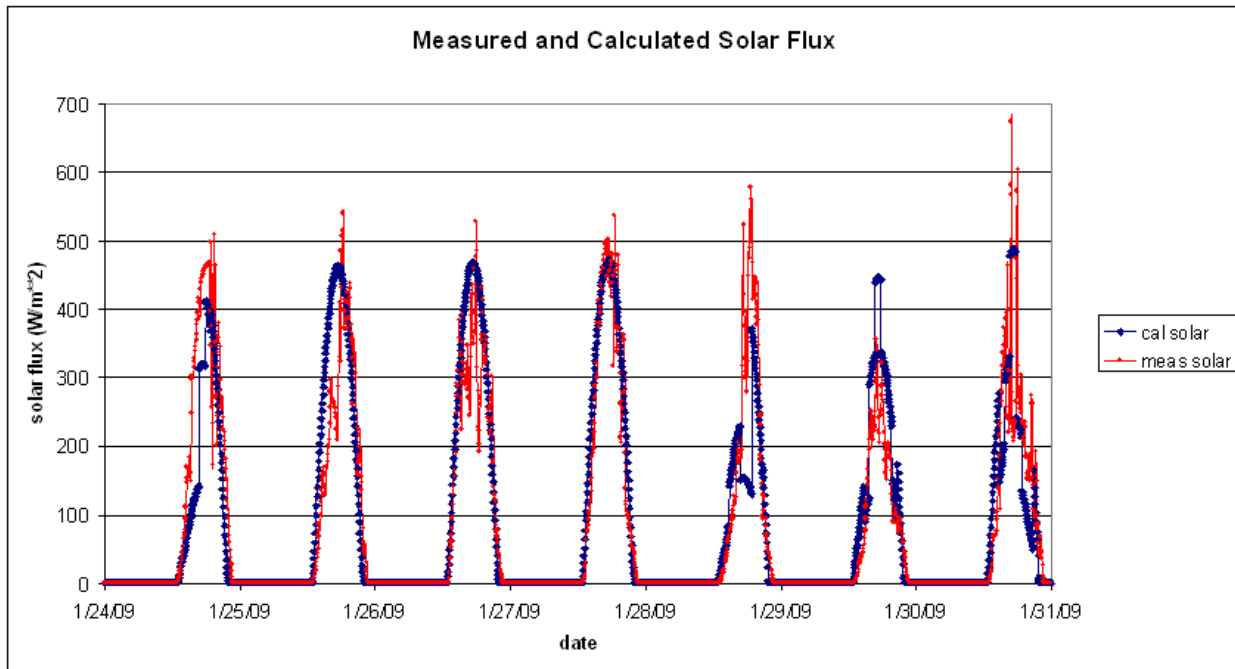


Fig. 8. Measured and calculated solar fluxes during late January 2009. Spiking in measured solar flux during midday is apparent on all but one day, but most obvious during the period January 25 – 27, when scattered clouds were present.

Figure 9 compares computed time series of ice cover for 5 simulations: baseline case with measured (100%) heat load (Q) from Midland power plant and 10 cm of snow cover, and same conditions but with 50%, 200%, 300% and 0% of heat load (Q). When there was no heat load (Q=0), the lake stayed completely ice covered during the entire winter season. Increasing Q to 300% greatly reduced the average amount of ice cover, but significant ice cover of about 50% was predicted during the coldest weather in January.

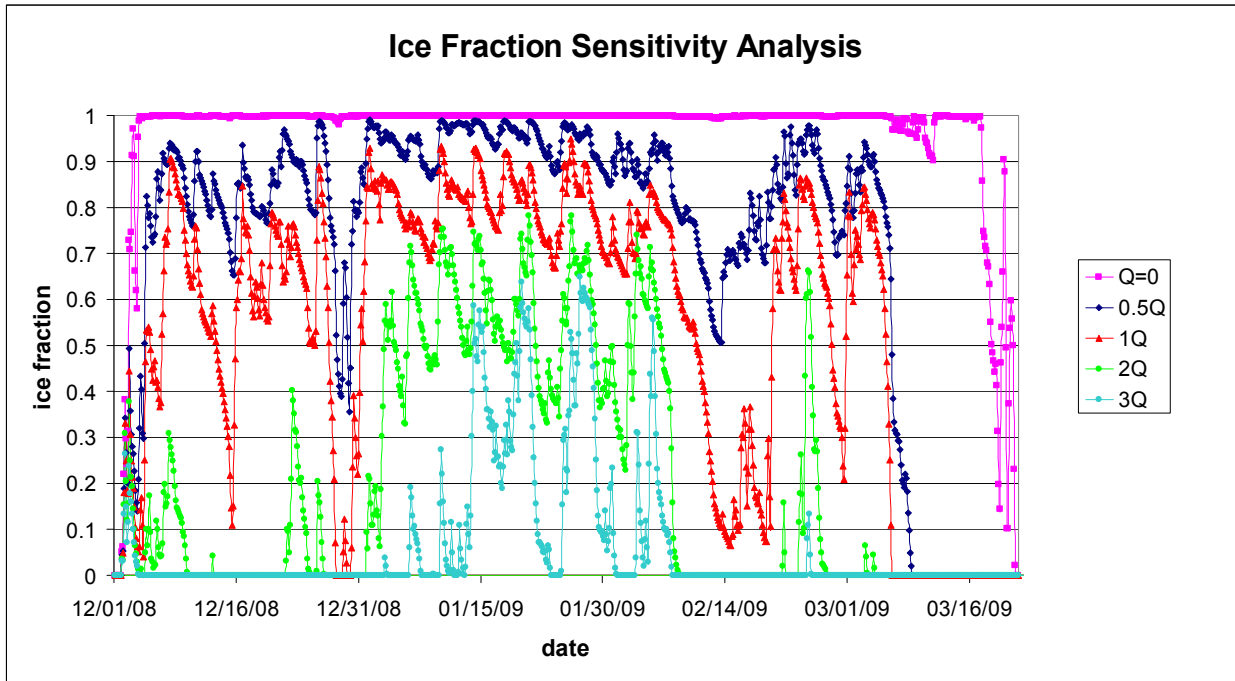


Fig. 9. Sensitivity of ice coverage to rate of heat discharge (Q) to lake. Q ranges from 0% of actual heat load to 50%, 100%, 200% and 300% of Q.

These results are summarized in Figure 10, which plots the relationship between Q and average ice cover. For the period from December 1, 2008 to March 22, 2009 the baseline simulation (Q = 100% of actual heat load) average ice cover is 56%. The 0% Q simulation produced an average ice cover of 96%, a 50% Q simulation produced an average ice cover of 75%; 200% Q simulation produced an average of 20% and 300% Q dropped the average ice cover down to 6%. Simulated ice cover thus ranges from near zero to almost 100% for the entire winter season when the heat load is varied by a factor of three.

The response of the simulated ice cover to the change in Q is large enough to indicate that average ice cover is a fairly robust indicator of average power. The relationship is also nearly linear. These results suggest that although ice formation and melting on a power plant cooling lake in a cold climate is a highly nonlinear combined 3-D hydrodynamic and thermodynamic problem, the relationship between average ice cover and Q and weather is fairly simple and nearly linear. The simplicity of the feedback between ice cover and Q may be attributable to the negative feedback loop between heat transfer from the lake to the atmosphere and ice cover. Ice drastically reduces evaporative and sensible heat losses from the lake surface to the air. So, as ice cover increases, the lake's ability to lose heat rapidly decreases, which drives the lake temperature up. As ice cover decreases, heat losses increase, which drops the lake temperature and prevents further decreases in ice cover. This feedback thus tends to stabilize the ice-cover at some intermediate value between ice-free and completely ice covered. This feedback may also explain why the simulated ice cover is fairly unresponsive to changes in snow cover (see Figure 3), i.e. snow cover affects only the ice-covered part of the lake, where heat transfer is small even without snow. For the period from December 1, 2008 to March 6, 2009 the average heat flux from the parts of the lake with no ice cover was 5.6 times larger than the average heat flux from the ice-covered parts of the lake. Thus, even though on the average 56% of the lake was covered by ice during the winter, the ice-covered part of the lake contributed only a small fraction of the total heat loss, and so its sensitivity to the insulating effect of snow cover was greatly reduced. The stabilizing negative feedback described here between ice-cover and heat loss from the lake surface is similar to a stabilizing feedback that has been postulated for Arctic Ocean ice cover¹¹.

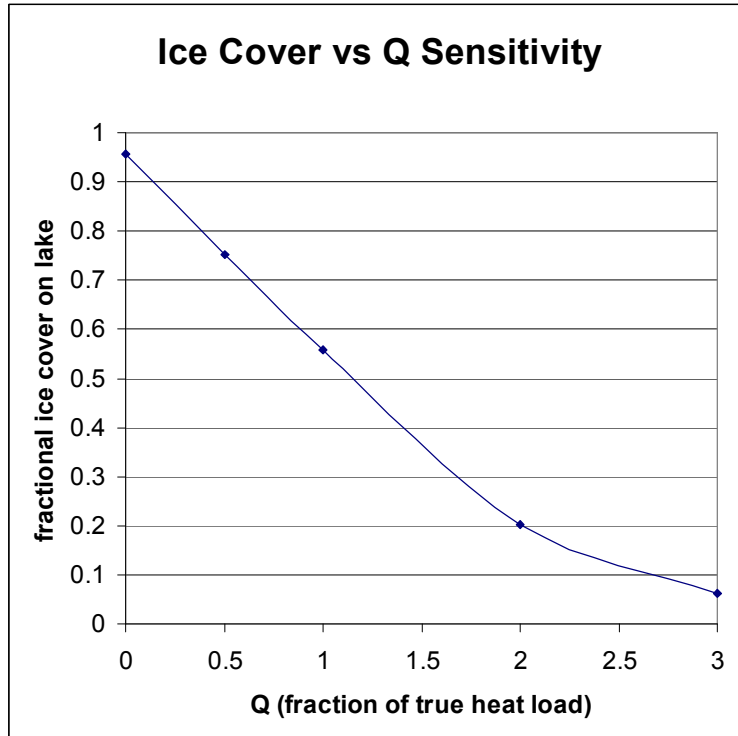


Fig. 10. Average simulated ice cover over MCV cooling lake as a function of Q.

The 5 instrumented buoys RIT deployed at different locations on the Midland cooling lake measured profiles of water and ice temperature that can be compared to ALGE simulations. Since these are point measurements (unlike the ice coverage, which is an integral quantity), the degree to which these data are representative of the part of the lake that they were located in is unknown. RIT found that the automated method for measuring ice thickness at Shiva and Surya stations often differed from hand measurements by 30 to 40%. The Shiva station was located fairly close to the cooling water intake, which is the coldest and iciest part of the lake. Figure 11 compares the time series of measured ice thicknesses at Shiva to the results of 4 simulations which used different combinations of 3 or 10 cm snow depth and empirical or one dimensional longwave radiation transfer 1D LWIR) models. The simulations that used 3 cm of snow produced the best agreement with measurements earlier in the time series but did worse than the simulations that used 10 cm of snow late in the simulations. Based on these results, it appears that simulated ice thickness is more sensitive to snow cover than the ice area, although the greater uncertainty of the automated ice thickness measurements and the fact that these are point measurements (rather than area-integrated) makes this conclusion more tentative. Unlike the ice cover results, the simulated ice thicknesses were not sensitive to the type of downwelling thermal radiation model.

Figure 11 shows that there was a sudden decrease in measured and simulated ice thickness at Shiva around February 9. This event was the result of a sudden increase air temperature from below freezing to about 5°C that was accompanied by strong winds. The strong winds increase the rate of transfer heat from the air to the ice surface, thus speeding the rate of melting. If the wind direction is from the warmer part of the lake to the colder (ice-covered) part of the lake, then a second mechanism acts to increase the rate of melting. In this situation, the winds increase the speed of the current that carries above freezing water underneath the ice. During the period from February 7 to 10, above-freezing air temperatures combined with strong winds to cause melting from above and below the ice layer. As a result, the measured ice thickness dropped to zero, and all 4 simulations predicted much thinner or no ice.

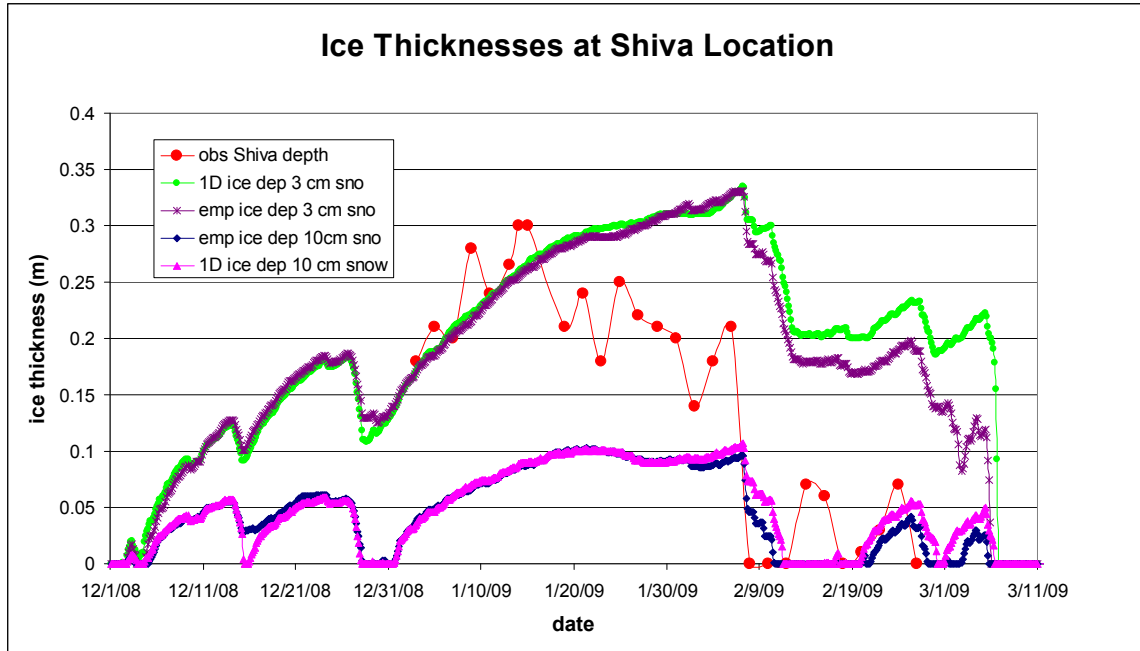


Fig. 11. Measured and simulated ice thicknesses at Shiva station during winter of 2008 – 2009. Results are plotted from four simulations using combinations of 3 cm and 10 cm snow thicknesses and empirical and 1D LWIR models. Sudden decreases in ice thickness (measured and simulated) about February 9 was caused by combination of warmer weather and strong winds.

Figure 12 shows an image created from one of the simulations during the February 7 – 10 period when the strong winds and above freezing air temperatures were causing rapid ice melting. Simulated surface current velocity vectors are plotted over temperature in Figure 12, to show the effect of the remaining ice on the surface water currents. Maximum computed surface current velocity was 0.44 m/s. The surface currents diverge around the remaining ice and are weaker below than they are in the open waters just upstream. The weaker currents underneath the ice are the result of the combined effect of frictional drag of the ice on the water just underneath and the shielding of the water under the ice from wind stress. In spite of the retarding effect of the ice on the surface currents, the strong winds forced above freezing water under the ice at a much higher rate relative to calm conditions, and accelerated the melting.

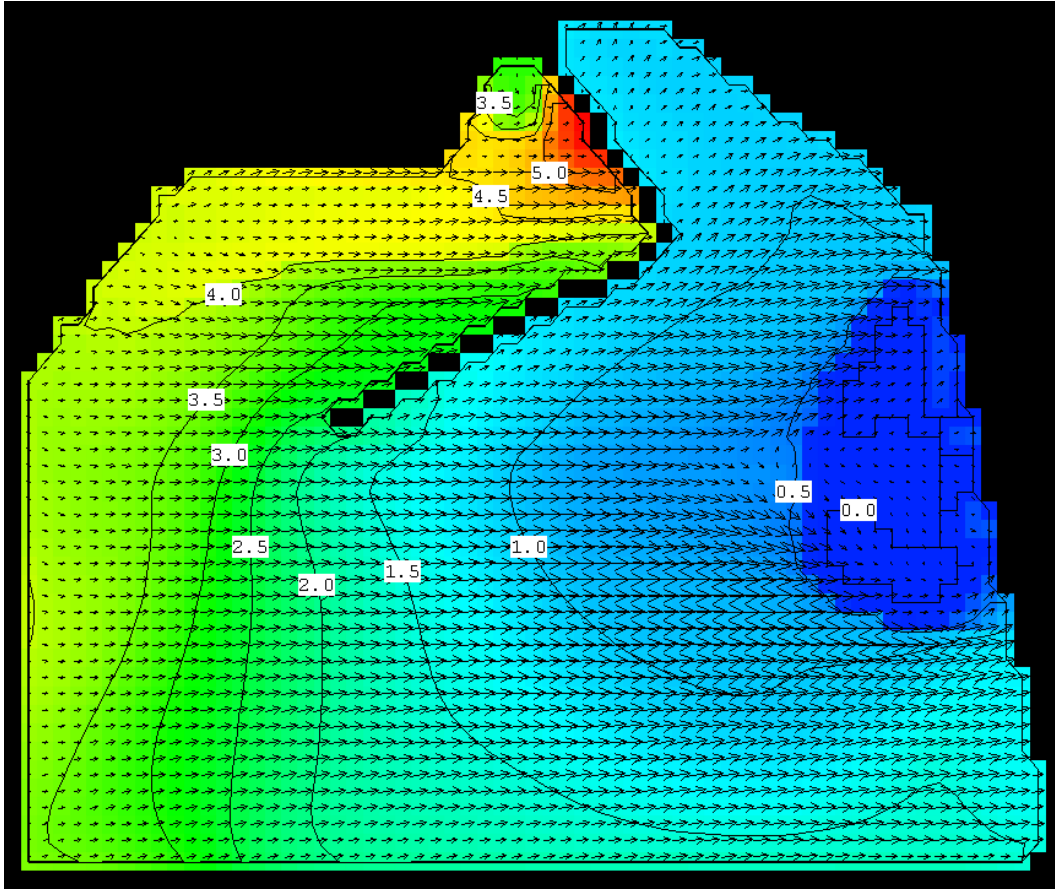


Fig. 12. Simulated surface temperatures and current velocities during the period February 7 – 10, 2009. Above freezing air temperatures and strong winds combined to cause rapid melting of remaining ice (dark blue area on right). Strong winds increased rate at which warmer water was brought into contact with underside of ice, thereby increasing the melting rate beyond what the warmer air would have accomplished.

SRNL has not completed comparisons of measured ice and water temperatures to ALGE simulations. Initial comparisons indicate discrepancies in some cases. Since these are point measurements, these data may not be completely representative of those variables away from the immediate vicinity of the sensor. SRNL and RIT will perform additional data analysis and model validation, with the 2008 – 2009 data set and the 2009 – 2010 data set.

4. SUMMARY

Research conducted by Savannah River National Laboratory (SRNL) and Rochester Institute of Technology (RIT) at the Midland Cogeneration Ventures (MCV) power plant near Midland, Michigan was directed toward improved understanding of the hydrodynamics and thermodynamics of cooling lakes operating in cold climates that produce partial freezing in winter. Visible, SWIR, MWIR and LWIR imagery was collected from aircraft and from elevated ground positions. The imagery allowed SRNL and RIT to observe ice formation and melting over the entire lake as a function of time, and to relate the transient ice cover to weather conditions and the rate of waste heat discharge from the power plant into the lake. SRNL used a 3-D hydrodynamic code with a full set of heat transfer equation sets and a validated ice model taken from published literature to simulate the MCV cooling lake during the fall, winter and early spring of 2008 – 2009. SRNL found that the transient ice cover could be accurately simulated in spite of the fact that there are large uncertainties in the depth and properties of the snow layer on top of the lake ice. Simulated ice depths and water and ice

temperature profiles were less accurate. These variables were ground-based, point measurements which may not have been as representative of conditions over large areas of the cooling lake as the space-integrated remote sensing data.

Ice formation and melting on the MCV cooling lake is highly variable because large but varying amounts of waste heat are being discharged into an extremely cold but variable atmosphere. The accuracy of the ice cover simulations appears to largely be attributable to a powerful negative feedback mechanism that arises from the large difference in rate of heat loss from liquid water versus ice. Heat loss rates from ice-covered surfaces are much less than from liquid water surfaces. For this reason, excessive ice cover for existing conditions inhibits heat transfer and the lake heats rapidly due to the waste heat input. This causes enough ice melting to increase the liquid water area and rate of heat loss to the atmosphere and a new quasi-equilibrium is reached. This negative feedback is equally powerful when existing ice cover is too small relative to meteorological conditions and heat load. The insensitivity of the simulated ice cover to snow depth is probably attributable to the much smaller heat losses over the ice-covered parts of the lake, which makes the specific snow depth over the ice in the simulations unimportant.

ACKNOWLEDGMENTS

This report was prepared for the United States Department of Energy under Contract No. DE-AC09-96SR18500. The authors would like to thank the personnel at the Midland Cogeneration Ventures plant for their support.

REFERENCES

- [1] Arsenovic, M. V. and Salvaggio, C., Garrett, A. J., Bartlett, B., Faulring, J., Kremens, R. and Salvaggio, P. "Use of remote sensing data to enhance the performance of a hydrodynamic simulation of partially frozen power plant cooling lake". Proc. SPIE, Vol. 7299, 72990B, (2009); doi:10.1117/12.818956. Online publication date: 22 April 2009.
- [2] Blanton JO, Garrett AJ, Bollinger JS, Hayes DW, Koffman LD, Amft J, 2009, "Transport and Dispersion of a Conservative Tracer in Coastal Waters with Large Intertidal Areas", *Estuaries and Coasts* **32**(3):573-592.
- [3] Garrett, A. J., "Analyses of MTI imagery of power plant thermal discharge," *Imaging Spectrometry VII* **4480**, pp. 264–273, SPIE, Jan 2002.
- [4] Garrett, A. J. and D. Hayes, "Cooling lake simulations compared to thermal imagery and dye tracers," *Journal of Hydraulic Engineering*, **123**, p. 885, 1997.
- [5] Garrett, A. J., J. M. Irvine, T. K. Evers, J. Smyre, A. D. King, C. Ford, D. Levine, 2000: An Imagery-Based Hydrodynamic Simulation of An Effluent Stream Entering the Clinch River. *Photogrammetric Engineering and Remote Sensing*. **66**, 329-335.
- [6] Li, Y., A. Vodacek, N. Raqueno, R. Kremens, A. J. Garrett, I. Bosch, J.C. Makarewicz, T.W. Lewis. Circulation and stream plume modeling in Conesus Lake. *Environmental Modeling and Assessment*, Published online April 21, 2007, doi: 10.1007/s10666-007-9090 x. (2007), Hardcopy journal publication: **13**, #2, 275 – 289, May, 2008.
- [7] Duguay, C. R., G. M. Flato, M. O. Jeffries, P. Menard, K. Morris, and W. R. Rouse, 2003: Ice-cover variability on shallow lakes at high latitudes: model simulations and observations. *Hydrol Process.*, **17**, 3465-3483.
- [8] Ebert, E. E. and J. A. Curry, 1993: An intermediate one-dimensional thermodynamic sea ice model for investigating ice-atmospheric interactions. *J. Geophys. Res.*, **98**, 10085-10109.
- [9] Maykut, G. A. and P. E. Church, 1973: Radiation climate of Barrow, Alaska, 1962 – 1966. *J. Appl. Meteor.*, **12**, 620–628.
- [10] Kondratyev, K. Ya., 1965: Radiation in the atmosphere. Pergamon Press.
- [11] Eisenman, I., and J. S. Wettlaufer, 2009: Nonlinear threshold behavior during the loss of Arctic sea ice. *Proceedings of the National Academy of Science*, **106**, #1, 28-32.